International Journal of GEOMATE, May 2023, Vol. 24, Issue 105, pp.1-10
ISSN: 2186-2982 (P), 2186-2990 (O), Japan, DOI: https://doi.org/10.21660/2023.105.3763
Geotechnique, Construction Materials and Environment

DISTRIBUTION OF THE SUBGRADE REACTION MODULUS FOR ANCHOR PILES WITH VARIOUS INCLINATION ANGLES

*Toshiya Oda[1] and Takashi Nagao[2]

[1] Port and Airport Group, Structure Division, Chuo Fukken Consultants Co., Ltd., Osaka, Japan
[2] Research Center for Urban Safety and Security, Kobe University, Kobe City, Japan

*Corresponding Author, Received:12 Dec. 2022, Revised: 18 Feb. 2023, Accepted: 12 March 2023

ABSTRACT: In a seismic design of a pile foundation, a subgrade reaction generated with a displacement of piles when the seismic load is applied must be appropriately evaluated. The ratio of the subgrade reaction to the amount of displacement of a pile is defined as the subgrade reaction modulus (SRM). There are two ideas about the SRM's depth distribution: one assumes a constant depth distribution, while another assumes a monotonously increasing depth distribution. There are various types of pile foundations based on different inclination angles of a pile. In design practice, SRM is not seen as being dependent on the pile type. In this study, we targeted anchor piles with the main goal of bearing a horizontal load and conducted a horizontal loading experiment. We prepared a model considering that anchor piles are usually not embedded into the bedrock and evaluated the depth distribution of SRM by changing the inclination angle of the pile from 0 to 30° with 10° intervals. The experimental result showed that though SRM increases monotonously in the depth direction, the distribution was different from what was assumed in design practice, where a local maximum was present at a specific depth in the ground, and the value decreased below that depth. We then proposed equations to calculate the degree of change in SRM corresponding to the inclination angle of a pile. Furthermore, it was shown that the position of a local maximum for SRM depends on the location of the rotational center for the pile.

Keywords: Subgrade reaction modulus; Anchor pile; Horizontal loading experiment; Seismic resistance

1. INTRODUCTION

A pile foundation is often used to bear a vertical load, such as the weight of a structure. Sufficient resistance to horizontal loads (e.g. seismic load), is required in a pile foundation. Piles with a goal of bearing vertical loads are usually embedded into the bedrock. Anchor piles are sometimes used in structures such as quays to resist horizontal loads; in such a case, there is little expectation for anchor piles to bear vertical loads. Therefore, anchor piles are not usually embedded into the bedrock. There are vertical and batter piles depending on the angle of placement. When the main goal is to bear vertical loads, vertical piles are often used; however, batter piles are superior in terms of resistance to horizontal loads. For example, [1-5] have experimentally and analytically shown the utility of batter piles as the foundation for piers.

When the seismic load is applied to a pile foundation, horizontal displacement occurs in the foundation and a subgrade reaction is generated to resist the seismic load. Seismic resistance of the vertical piles is exerted through a combination of the flexural rigidity of the piles and subgrade reaction, where the axial bearing capacity of the piles barely contributes to the seismic resistance. Meanwhile, when there is a horizontal load on a battered pile, part of the horizontal load is in the axial direction, and the only load perpendicular to the pile axis is borne by the flexural rigidity of the pile and subgrade reaction. As such, the resistance mechanism against horizontal loads is different for vertical and batter piles; but in both cases, subgrade reaction must be accurately assessed for a seismic design of a pile foundation. The ratio of subgrade reaction to pile displacement is defined as subgrade reaction modulus (SRM). Methods of calculating SRM shown in the literature and various design codes are roughly divided into methods based on the relative density of the ground [6,7] and methods based on the deformation modulus of the ground [8,9]. For the depth distribution of SRM, there are cases where SRM is considered to be constant in the depth direction [9] and cases where it is assumed to increase monotonously [10,11]. In design practice, depth distribution is usually considered to be constant for its ease; however, considering its distribution to be monotonously increasing in the depth direction can more accurately assess the actual subgrade reaction [9]. As such, there are various ideas of ground parameters used for SRM calculations and depth distribution; however, the depth distribution of SRM is assumed not to change according to the above-mentioned pile types.

There have been many horizontal loading experiments and shaking table experiments conducted on pile foundations installed in a soil tank. Conditions for the pile tip include the one in which the tip is fixed to the soil tank [12-16] and the one where the tip is installed in the ground [10,17-20]. As an experiment noticing the bearing capacity of a pile, there are cases in which the lower end of a pile is installed in the ground [21]. With the former condition, it is relatively easy to perform an experiment, but the deformation of a pile caused by a horizontal load or shaking is limited to bending deformation. Meanwhile, with the latter condition, it is not limited to the bending deformation of a pile, and a horizontal load and shaking can also cause translation and rotation. As discussed above, anchor piles with the main goal of bearing horizontal loads are usually not embedded into the bedrock; thus, there is a displacement at the pile tip due to the horizontal load. If the pile tip is fixed to the soil tank, the response will be different from the actual behavior of piles. Regarding the installation angle of piles, previous studies mostly targeted vertical piles. Though there is a study that examined group piles (a combination of batter and vertical piles) [18], there is no study that only examined a single batter pile.

In the present study, we focused on an anchor pile with the goal of resisting a horizontal load and conducted a horizontal loading experiment to evaluate the impact of different inclination angles of the pile on the depth distribution of SRM. The inclination angle of the pile was changed from 0 to 30° in 10° intervals. As the bearing of the vertical load was not the goal, the pile tip was not fixed to the soil tank. Piles are classified into end bearing, friction, vertical, batter, and long and short based on the flexural rigidity of a pile and embedded length. The above-discussed experiments [10,18] targeted long piles, but we used a short pile. Most previous studies obtained the bending moment of piles from strain values measured by a strain gauge attached to a pile, from which subgrade reaction was calculated by taking a second derivative [12-15,17]. One of those studies assessed the depth distribution of subgrade reaction [15], but the strain on a pile was small in depth; thus, the measured value and subgrade reaction calculated from the value are both not quite reliable. There is a study that measured subgrade reaction by attaching an earth pressure gage on a pile [22], but there have been few reports that examined the depth distribution of SRM along with subgrade reaction based on the measurements taken with an earth pressure gage. Thus, in the present study, we attached an earth pressure gauge to the pile and directly measured the subgrade reaction. Based on the displacement of the pile and subgrade reaction, we assessed the depth distribution of SRM and discussed the difference from the depth distribution of SRM used in previous studies and design codes.

2. RESEARCH SIGNIFICANCE

There are various types of pile foundations depending on the difference in the inclination angle of the pile (vertical pile and battered pile); in design practice, subgrade reaction modulus (SRM) is regarded to be independent of the pile type. In this study, a horizontal loading model test was conducted by changing the inclination angle of the pile, and the depth distribution of SRM was evaluated. This study clarified the quantitative degree of change in SRM due to the inclination angle of the pile. This allows SRM to be set according to the inclination angle in design practice.

3. METHOD

3.1 Outline

We used soil tank dimensions of 880 mm wide, 500 mm deep, and 500 mm high (Fig.1). Four cases with different initial inclination angles for the pile were examined (Table 1). Loading was conducted using a mega torque motor. A steady brace was attached to prevent the pile from leaning in the depth direction of the soil tank. To meet the condition in which the pile tip is not fixed to the soil tank, we placed the pile after pouring sand up to the height of 100 mm from the tank bottom. Tohoku Silica sand no. 6 was used in a dry state. Air pluviation method was used so that the relative density (D_r) would be approximately 75%. Fig.2 shows the setup for the pile with Case 3 as an example. To minimize the impact of the soil tank on the subgrade reaction, we installed the pile at 730 mm from a soil tank wall in the direction in which the pile head is displaced. After installing the pile, we poured sand to the height of 450 mm from the soil tank bottom.

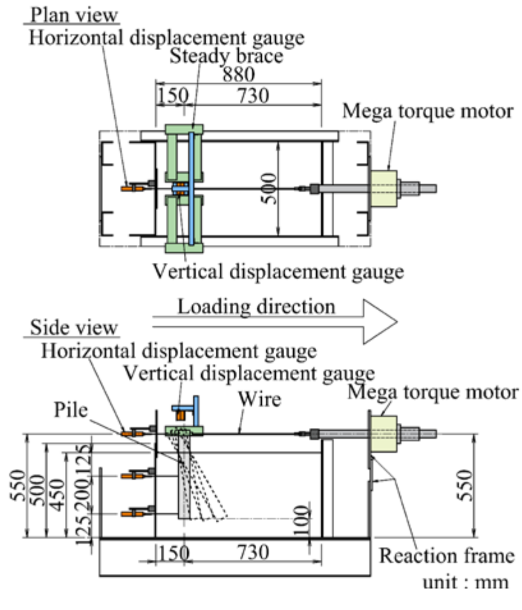

Fig.1 Experimental apparatus

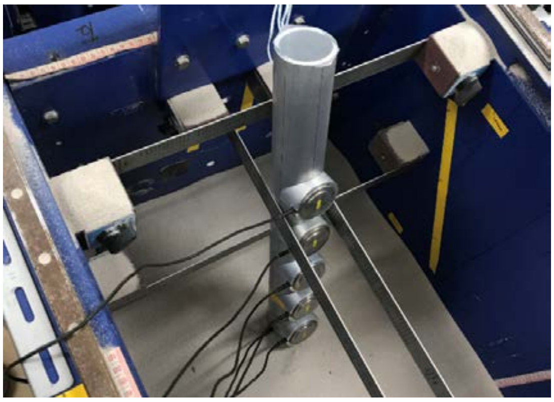

Fig.2 Pile setup (Case 3)

Table 1 Examined cases

	Initial inclination angle
Case 1	0
Case 2	10°
Case 3	20°
Case 4	30°

Specifications of the pile are shown in Table 2. We assumed 18 m for the actual pile length and set the scale ratio of the length at 40 (actual pile/model pile) by considering the size of the soil tank. For the actual pile, we assumed an outer diameter of 2,400 mm and a thickness of 8.0 mm and chose the outer diameter of 60 mm for the model pile based on the scale ratio. We applied the similitude for the shaking table experiment in 1g gravitational field [23] and set the pile thickness so that the flexural rigidity would be the same for the actual pile and model pile. The loading speed in the experiment was 0.5 mm/s, while the maximum horizontal displacement of the pile head was at least 20 mm. According to the similitude, the loading speed in the real scale would be 7.95 cm/s, while the maximum horizontal displacement of the pile head would be over 5 m.

Table 2 Pile specifications

Diameter (mm)	60.0
Thickness (mm)	5.0
Young's modulus (kN/m^2)	7.00×10^{7}
Cross-sectional area (m^2)	8.64×10^{-4}
Moment of inertia of area (m^4)	3.29×10^{-7}
Flexural rigidity (kNm^2)	2.31×10

3.2 Measured Items

Items measured in this experiment were (1) load, (2) horizontal displacement, (3) vertical displacement, and (4) subgrade reaction at the front side of the pile. We used a data logger to record the time history data of all items. Hereafter, we consider the direction of the displacement for the pile head as the front side of the pile and the opposite side as the backside of the pile.

Taking Case 4 as an example, we presented the attachment position of each measuring instrument in Fig.3. The values of horizontal displacement, vertical displacement, and earth pressure were shown as x, y, and Ep, respectively, and the number was added as shown in the figure. With the top, center, and bottom of the pile as the targets, the displacement gauge and the backside of the pile were connected with a wire to measure the horizontal displacement. By passing the wire through a sleeve, we eliminated the friction between the ground and the wire. The position of the horizontal displacement measurement for the center and the bottom of the pile was 225 mm and 25 mm from the pile tip, respectively. Meanwhile, the position of the horizontal displacement measurement for the pile head varied based on the initial inclination angle of the pile. For the vertical displacement, we used a laser-type displacement gauge fixed to the soil tank to measure the distance to the supplement plate attached to the pile head. Measurements were taken at two locations with a 30 mm interval in the horizontal direction. Subgrade reaction was measured at the pile tip and five heights from the tip—35, 105, 175, 245, and 315 mm—using an earth pressure gauge installed with a jig (Fig.2).

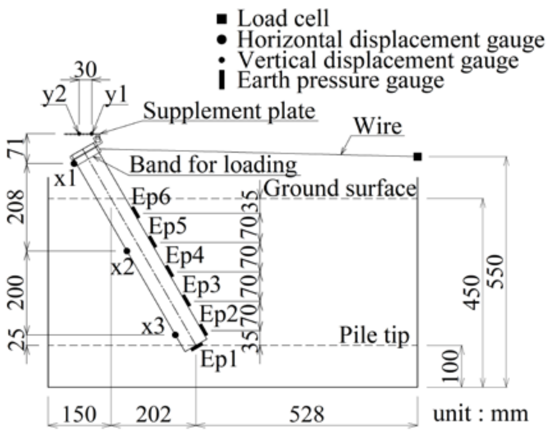

Fig.3 Attachment position for the measuring instruments (Case 4)

Measured values of subgrade reaction fluctuated greatly since sand particles repeatedly came in contact with the earth pressure gauge during loading, including a large number of high-frequency components. Thus, we performed a fast Fourier transform of the measured data and used a low-pass filter at 0.8 Hz. Then we performed the inverse Fourier transform to obtain the time history data [24,25]. Fig.4 shows the time history data for the values measured by the earth pressure gauge and values after filtering for Ep4 of Case 1 as an example. The gray line shows the measured values, while the red line shows the values after filtering.

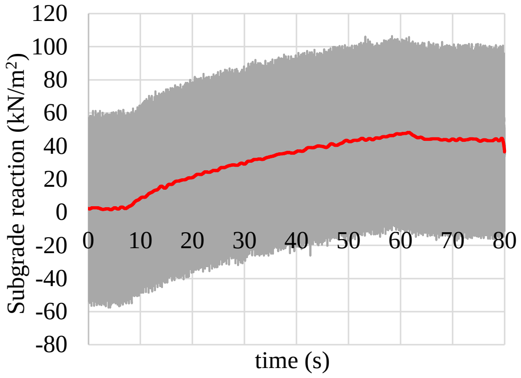

Fig.4 Example of filtering process (Case 1 Ep4)

4. RESULTS

4.1 Horizontal Displacement

Fig.5 shows the time history of the horizontal displacement of the pile in Case 1. Displacement in the load direction is positive. While x1 and x2 were displaced in the load direction, x3 was displaced in the opposite direction to the load. Each displacement became constant during loading because the horizontal displacement reached the measurement limit of the displacement gauge. Fig.6 showed the horizontal displacement distribution of the pile when the horizontal displacement of the pile head became 6 mm. As described above, the measurement height of x1 varied between cases; thus, hereafter, we consider the height of 450 mm from the pile tip as the pile head. At the end of loading, the pile maintained a linear shape in all cases: there was no bending deformation of the pile. The pile tip was displaced in the opposite direction to the load, where the pile rotated with a certain depth at the center. Rotation was the dominant deformation mode in this experiment.

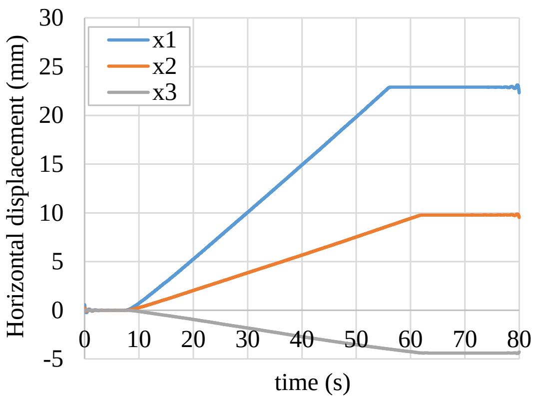

Fig.5 Time history of the horizontal displacement of the pile (Case 1)

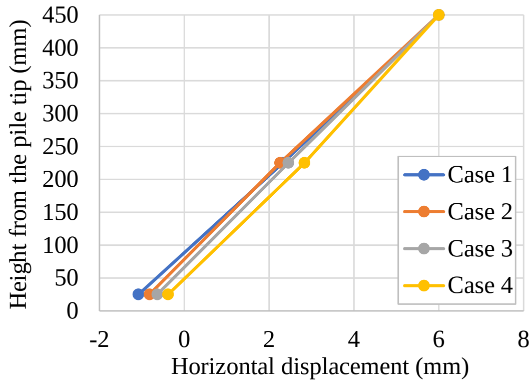

Fig.6 Horizontal displacement distribution for the pile (at the time of 6-mm displacement for the pile head)

4.2 Height of the Rotational Center

We used the measured values for x1 and x3 to obtain the height of the rotational center for the pile. Fig.7 shows the relationship between the initial inclination angle and the height of the rotational center. Values in the legend show the amount of horizontal displacement for the pile head. As the initial inclination angle of the pile increased, the height of the rotational center clearly decreased. The height of the rotational center did not depend on the amount of pile head displacement.

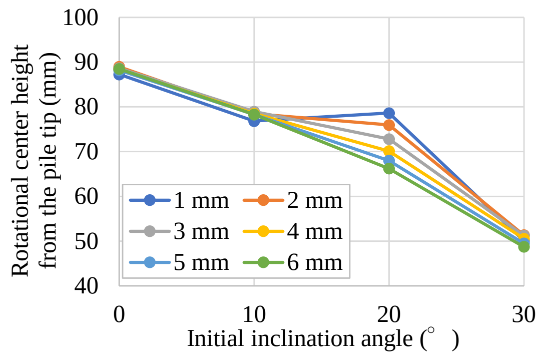

Fig.7 Relationship between the initial inclination angle and height of rotational center for the pile

4.3 SRM

Taking Case 1 as an example, we demonstrated the relationship between the horizontal displacement of the pile head and subgrade reaction (Fig.8). At Ep1, it dramatically decreased while the pile head displacement was small, reaching 0 when the displacement became 3 mm. Before loading, the weight of the pile created a subgrade reaction of 10.6 kN/m^2. However, with loading, the pile rotated, where the pile tip was no longer in contact with the ground; thus, the subgrade reaction was no longer measured. Ep2 was located below the rotational center for the pile; displacement was opposite to the load direction. Thus, there was no subgrade reaction on the front side of the pile. Ep3 was close to the rotational center, and displacement was small. The subgrade reaction barely changed. In contrast, Ep4 to Ep6 was far from the rotational center, experiencing a notable displacement in the load direction; thus, the subgrade reaction increased with the increase in the horizontal displacement of the pile head. Note that Ep6 was located near the ground surface where the confining pressure of the ground was extremely small; thus, as the horizontal displacement of the pile head increased, the ground in front of the pile was raised and shifted toward the backside of the pile around the circumference of the pile. This makes the compression of the ground less likely, limiting the increase in subgrade reaction.

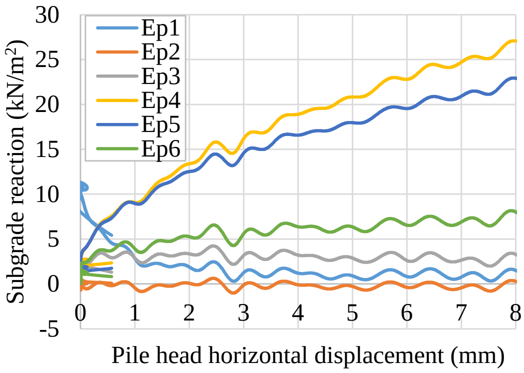

Fig.8 Relationship between the horizontal displacement of the pile head and subgrade reaction (Case 1)

Subgrade reaction and the horizontal displacement of the pile at a certain depth can be expressed with Eq. (1).

$$p = ky \tag{1}$$

where p is the subgrade reaction (kN/m^2), y is the horizontal displacement of the pile (m), and k is the SRM (kN/m^3).

Based on Eq. (1), we calculated SRM at a depth of each earth pressure gauge. Fig.9 shows the relationship between the horizontal displacement of the pile head and SRM. Regardless of the initial inclination angle of the pile and depth, due to the impact of the nonlinear property of the soil and soil slipping past around the pile circumference, SRM decreased as the horizontal displacement increased. Up to 1 mm of pile head horizontal displacement (25 cm in the actual scale), SRM rapidly decreased. When it exceeded 2 mm (50 cm in the actual scale), SRM did not change significantly. A similar phenomenon has been identified for vertical SRM that works on the bottom surface of a wide foundation [26].

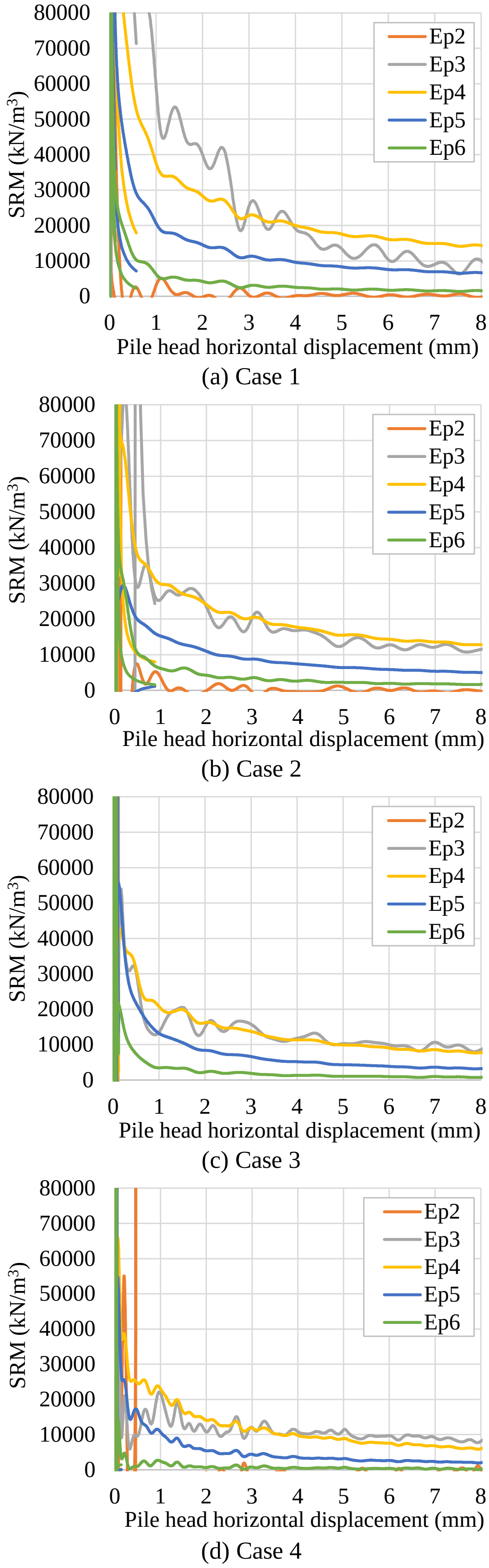

Fig.9 Relationship between pile head horizontal displacement and SRM

With Ep4 to Ep6, where subgrade reaction increased with the horizontal displacement of the pile head as the target, we show the relationship between the initial inclination angle of the pile and SRM when the horizontal displacement of the pile head was 6 mm (Fig.10). Here SRM ratio that has been normalized with the SRM of Case 1 is shown. We also show the approximation curve of the SRM ratio obtained with a quadratic function using a solid line. At Ep4 and Ep5, as the initial inclination angle increased, the SRM ratio linearly decreased. Meanwhile, the SRM ratio of Ep6 with little confining pressure was constant when the initial inclination angle was in the range of 0–10°, but rapidly decreased when the initial inclination angle was in the range of 10°–30°.

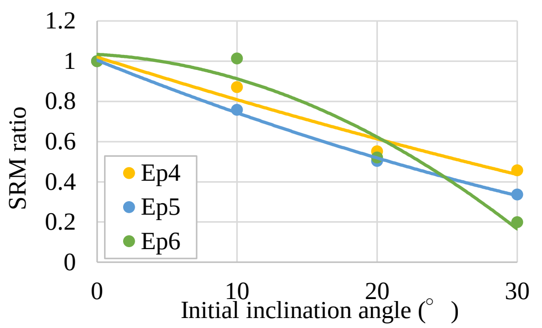

Fig.10 Relationship between initial inclination angle and SRM ratio (at the time of 6-mm displacement for the pile head)

With the point at which the horizontal displacement of the pile head was 6 mm as an example, we show subgrade reaction distribution and SRM distribution in Figs.11 and 12, respectively. As discussed, we were unable to obtain subgrade reaction at Ep2; thus, we only targeted values for Ep3 to Ep6. At the rotational center, there was no displacement in a pile; thus, we set the subgrade reaction at the height of the rotational center as zero. The shape of SRM distribution varied between each case.

5. DISCUSSIONS

5.1 Comparison with Various Design Codes for SRM

Various design codes indicate various assessment methods for SRM, and these can be roughly divided into methods that are based on the relative density of the ground [6,7] and methods that are based on the deformation modulus of the ground [8,9]. As for the depth distribution of SRM, there are cases where it is considered to be constant in the depth direction [9] and cases where it increases monotonously [10,11]. In the present study, we define each method in Table 3.

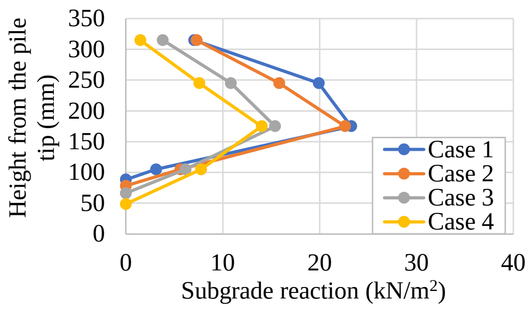

Fig.11 Subgrade reaction distribution (pile head displacement of 6 mm)

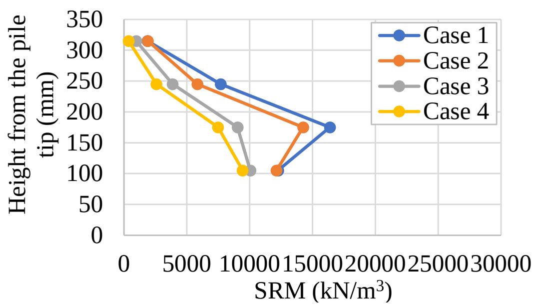

Fig.12 SRM distribution (pile head displacement of 6 mm)

Table 3 Method to evaluate SRM

Depth direction distribution / Soil property	Constant (C)	Increase (I)
Relative density (RD)	RD-C	RD-I
Deformation modulus (DM)	DM-C	DM-I

RD-I includes a method that obtains SRM with Eq. (2) [7]. The rate of increase for SRM (n_h) shows the values corresponding to relative density (Table 4).

$$k = n_h x / B \tag{2}$$

where k is the SRM (kN/m^3), n_h is the rate of increase for SRM, the value shown in Table 4 (kN/m^3), x is the depth (m), and B is the pile width (m).

Table 4 Rate of increase for SRM (n_h) [7]

Relative density of sand	Loose	Intermediate	Dense
Dry or wet sand	2200	6600	17600
Sand in water	1300	4400	10800

Note: Unit is kN/m^3

DM includes a method that obtains SRM with Eq. (3) [8].

$$k = \lambda k_0 (B'/0.3)^{-3/4} \tag{3}$$

where λ is the coefficient that considers the impact of the construction method of the foundation, k_0 is the SRM (kN/m^3) equivalent to the value of the plate loading test using a rigid disk with a diameter of 0.3 m ($k_0 = \alpha\ E\ /\ 0.3$), E is the deformation modulus of the ground (kN/m^2), α is the conversion coefficient for SRM, and B' is the converted loading width (m) of the foundation used to estimate SRM.

In terms of Eq. (3), it has been suggested that it overestimates the SRM dependency on the foundation width [27], but in the present study, the pile width was not changed and we focused on the depth distribution of SRM. Thus, we used Eq. (3) as is. The average deformation modulus of the ground was determined to be 2,000 kN/m^2 from a separate compression experiment. Meanwhile, for the DM-I type, the shear modulus of the ground was proportional to the 0.5 power of the effective confining pressure [28] and the deformation modulus and the shear modulus of the ground were in the proportional relationship shown in Eq. (4); and thus, we considered the deformation modulus of the ground to be proportional to the 0.5 power of the effective confining pressure.

$$E = 2(1 + \nu)G \tag{4}$$

where G is the shear modulus of the ground (kN/m^2) and ν is the Poisson's ratio of the ground.

A comparison of the SRM distribution when the horizontal displacement of the pile head was 6 mm is shown in Fig.13. None of the existing calculation methods show a local maximum for SRM at a certain depth. In most of the previous studies, as with the design codes, SRM is regarded as monotonically increasing in the depth direction [29,30], or it is regarded as a constant value in the depth direction [30,31]. In contrast, [32] performed a finite element analysis, showing SRM of decreasing depth-wise after increasing monotonically to a certain depth. The finding is consistent with the result of this study. Since the pile displaced toward the backside below the rotational center, there was a gap between the ground and the front side of the pile into which surrounding and above—ground shifted to fill the gap. For this reason, sand at the front side of the pile right above the rotational center became loose. Therefore, even if the pile was displaced, there was almost zero subgrade reaction, and SRM began to show a decreasing trend at a certain depth above the rotational center.

As Fig.13 connects the SRM assessed at the installation positions of the earth pressure gauge with a straight line, the height of the local maximum for SRM is unclear. Thus, we obtained an approximation curve for the subgrade reaction distribution through spline interpolation and obtained the SRM distribution by dividing the subgrade reaction distribution by horizontal displacement at each depth. Fig.14 shows the SRM distribution obtained in this manner for examples where the horizontal displacement of the pile head was 2 and 3 mm. The height of the local maximum for the SRM in each case is shown with a dashed line. In Case 1 where the pile head displacement was small (1–2 mm), the SRM linearly increased in the depth direction and reached its maximum at the rotational center, which is in harmony with the existing idea. Given the similitude, it is equivalent to about 50 cm or less on the real scale. Meanwhile, when the pile head displacement in Case 1 reached 3 mm or more (75 cm or more in the real scale), or in Cases 2–4, the SRM reached its local maximum at a certain depth in the ground and then began decreasing; the SRM distribution diverts from that of design practice.

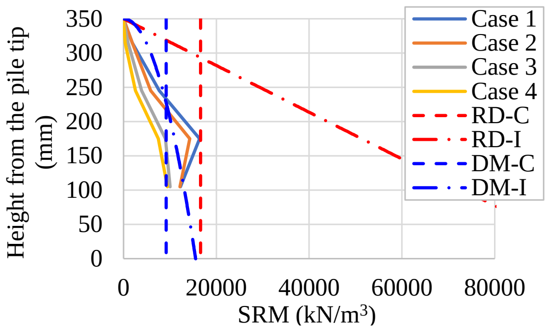

Fig.13 Comparison of SRM distribution (at the time of 6-mm displacement for the pile head)

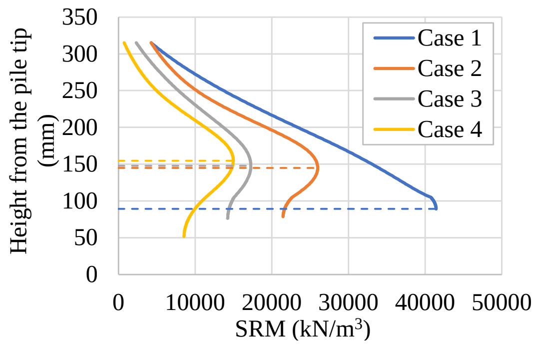

(a) Pile head displacement of 2 mm

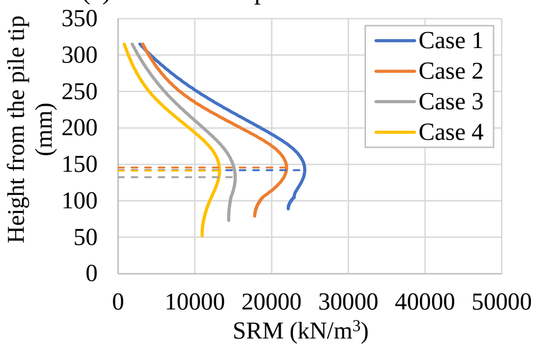

(b) Pile head displacement of 3 mm

Fig.14 Approximation curve of SRM distribution

5.2 SRM Ratio

As was pointed out in the design code [9], SRM decreases more with an increase in the initial inclination angle. However, there has been no comprehensive examination of the degree of decrease in SRM corresponding to the inclination angle of the pile. Fig.15 shows the relationship between the initial inclination angle of the pile and the SRM ratio obtained from SRM at the height of 150 mm from the pile tip for cases where the horizontal displacement of the pile head was 2 and 3 mm. The horizontal displacement of the pile head of 2 mm is equivalent to 50 cm in the real scale, which is in the range of pile head displacement considered in design practice when the reference ground motion is relatively small. The SRM ratio rapidly decreased when the initial inclination angle was 0–20° but became mostly constant when the initial inclination angle was 20°–30°. Eq. (5) was obtained from an approximation that used a quadratic function. Meanwhile, pile head displacement of 3 mm is equivalent to 75 cm of displacement in the real scale, which corresponds to displacement during a massive earthquake. In this range, as the initial inclination angle increased, the SRM ratio linearly decreased, where Eq. (6) was obtained from linear approximation.

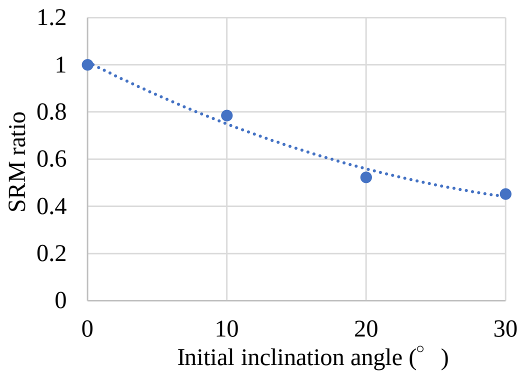

(a) Pile head displacement of 2 mm

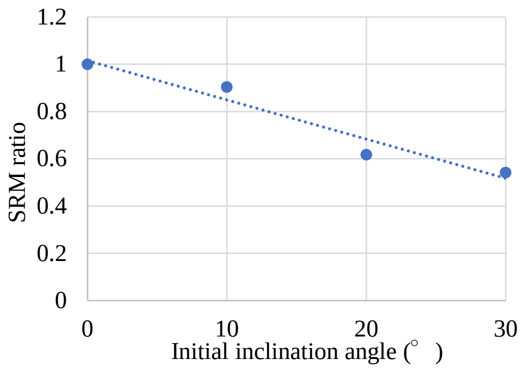

(b) Pile head displacement of 3 mm

Fig.15 Relationship between initial inclination angle of pile and SRM ratio

$$rSRM = 0.0004\theta^2 - 0.0299\theta + 1.0120 \qquad (5)$$

$$rSRM = -0.0166\theta + 1.0152 \qquad (6)$$

where *rSRM* is the SRM ratio and θ is the initial inclination angle of the pile (°).

5.3 Height of SRM Local Maximum

Fig.16 shows the relationship between the SRM local maximum height and the initial inclination angle of the pile. When the pile head displacement was small, excluding Case 1, the difference in the SRM local maximum height was limited. However, when the pile head displacement became large, the difference in the SRM local maximum height due to the initial inclination angle of the pile became notable, where larger initial inclination angles led to lower SRM local maximum height. When the pile head displacement was 3 mm, the difference in the SRM local maximum height was 13 mm; however, when the displacement reached 6 mm, the difference was significant, at 53 mm. Fig.17 shows the relationship between the height of the rotational center of the pile and the SRM local maximum height. As the rotational center height increased, the SRM local maximum height increased linearly. The ratio of this increase was larger when pile head displacement was larger.

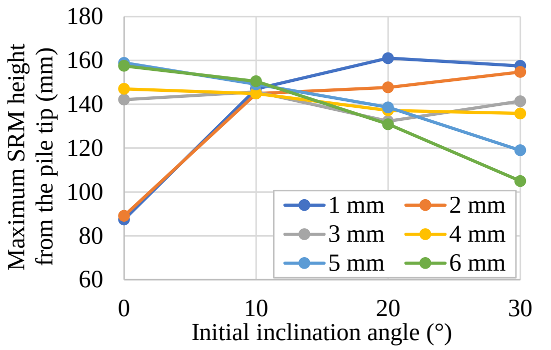

Fig.16 Relationship between the initial inclination angle of the pile and SRM local maximum height

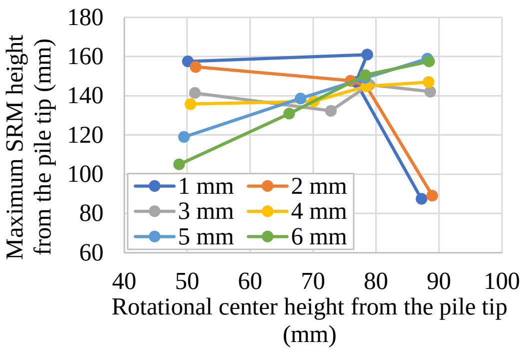

Fig.17 Relationship between the rotational center height and SRM local maximum height

6. CONCLUSIONS

In this paper, we conducted a horizontal loading experiment of four cases with different initial pile inclination angles. We assessed changes in the depth distribution of SRM and showed a relationship between the rotational center height and the SRM local maximum height. Major conclusions drawn from the study are as follows:

(1) Within the range of pile head displacement of 50 cm or less in the real scale for a vertical pile, the SRM linearly increased in the depth direction. Such SRM distribution is consistent with that of design practice. In contrast, with a batter pile or a vertical pile with a pile head displacement of 75 cm or more in the real scale, the SRM linearly increased to a certain depth, reached a local maximum, and then decreased. This phenomenon is not considered in design practice.

(2) When the pile head displacement was 50 cm or less in the real scale, the SRM ratio rapidly decreased when the initial inclination angle was 0–20° but became almost constant when the initial inclination angle was 20°–30°. Meanwhile, when the pile head displacement was 75 cm or more in the real scale, as the initial inclination angle increased, the SRM ratio decreased linearly. Based on these results, we proposed equations to estimate the degree of decrease in SRM in accordance with the initial inclination angle of the pile.

(3) With larger initial inclination angles of the pile, the height of the rotational center decreased. Similarly, the SRM local maximum height decreased with increasing initial inclination angle, where this tendency became more noticeable with a larger pile head displacement. As the rotational center height increased, the SRM local maximum height increased linearly. The larger the pile head displacement the larger the ratio of this increase was.

7. REFERENCES

[1] Roth W.H., Fong H. and Rubertis C., Batter piles and the seismic performance of pile-supported wharves, Proceedings of Ports’92, ASCE, Seattle, WA, 1992, pp. 336-349.

[2] Schlechter S.M., Dickenson S.E., McCullough N.J. and Boland J.C., Influence of batter piles on the dynamic behavior of pile-supported wharf structures, Ports Conference 2004, 2004, pp. 1-10, DOI: 10.1061/40727 (2004) 12.

[3] Razavi S.A., Fakher A. and Mirghaderi S.R., An insight into the bad reputation of batter piles in seismic performance of wharves, 4th International Conference on Earthquake Geotechnical Engineering, Paper No. 1423, 2007, pp. 1-10.

[4] Li J., Song B. and Cui J., Seismic dynamic damage characteristics of vertical and batter pile-supported wharf structure systems, Journal of Engineering Science and Technology Review, Vol. 8, No. 5, 2015, pp. 180-189, DOI: 10.25103/jestr.085.23.

[5] Li J., Song B. and Wu P., Comparative study of seismic dynamic damage on vertical and batter pile-supported wharf structures, Journal of Building Structures, Vol. 37, No. 7, 2016, pp. 151-157, DOI: 10.14006/j.jzjgxb.2016.07.019.

[6] American Petroleum Institute, Recommended Practice for Planning, Designing and Constructing Fixed Offshore Platforms - Working Stress Design, 2000, pp. 1-226.

[7] Terzaghi K., Evaluation of Coefficient of Subgrade Reaction, Geotechnique, Vol. 5, No. 4, 1995, pp. 41-50.

[8] Japan Road Association, Specifications for highway bridges, Part 4, substructures, Maruzen Co., Ltd., 2016, pp.1-569.

[9] Ports and Harbours Bureau, Ministry of Land, Infrastructure, Transport and Tourism, National Institute for Land and Infrastructure Management, Port and Airport Research Institute, Technical standards and commentaries for port and harbour facilities in Japan, The Overseas Coastal Area Development Institute of Japan, 2020, pp. 1-2182.

[10] Kubo K., A New Method for the Estimation of Lateral Resistance of Piles, Report of Port and Harbour Technical Research Institute Ministry of Transportation, Japan, Vol. 2, No. 3, 1964, pp. 1-37.

[11] Reese L.C. and Matlock H., Non-dimensional Solutions for Laterally Loaded Piles with Soil Modulus Assumed Proportional to Depth, Proc. 8th Texas Conf. SMFE, The Univ. of Texas, Austin, Paper No. 7, 1956.

[12] Dash S.R. and Bhattacharya S., Pore Water Pressure Generation and Dissipation near to Pile and Far-Field in Liquefiable Soils, International Journal of GEOMATE, Vol. 9, No. 18, 2015, pp. 1454-1459.

[13] Ibrahim S.F. and Hatem M.K., Behavior of Model Group Piles Subjected to Lateral Soil Movement in Sand, International Journal of GEOMATE, Vol. 14, No. 44, 2018, pp. 33-38.

[14] Funahara H., Components of Dynamic Subgrade Reaction on Pile in Saturated Sand, Geotechnical Earthquake Engineering and Soil Dynamics Congress IV, 2008, pp. 1-10, DOI: 10.1061/40975(318)80.

[15] Kavand A., Haeri S.M., Raisianzadeh J., Meibodi A.S. and Soltani S.A., Seismic

behavior of a dolphin-type berth subjected to liquefaction induced lateral spreading: 1g large scale shake table testing and numerical simulations, Soil Dynamics and Earthquake Engineering, Vol. 140, 2021, 106450, pp. 1-23.

[16] Karkush M.O. and AbdulKareem M.S., Behavior of Pile Group Subjected to Cyclic Lateral Loading in Contaminated Soils, International Journal of GEOMATE, Vol. 10, No. 21, 2016, pp. 1943-1949.

[17] Purnama A.Y., Yasufuku N. and Rifa'i A., Evaluation of Filler Material Behavior in Pre-Bored Pile Foundation System due to Slow Cyclic Lateral Loading in Sandy Soil, International Journal of GEOMATE, Vol. 16, No. 58, 2019, pp. 90-96.

[18] Muthukkumaran K. and Kumar B.A., Effect of Raker Piles in Lateral Load Capacity of Laterally Loaded Pile Group, Geotechnical Special Publication, Geo-Shanghai 2014, 2014, pp. 776-785, DOI: 10.1061/9780784413388.081.

[19] Gunawan S., Surjandari N.S., Setiawan B. and Purwana Y.M., Horizontal Movement of Pile Foundation due to Combined Loads, International Journal of GEOMATE, Vol. 22, No. 93, 2022, pp. 20-27.

[20] Lee J.H., Do J.U. and Kim S.R., A Comparative Study on the Resistances of Bucket Foundation in Sand with Different Installation Methods, International Journal of GEOMATE, Vol. 8, No. 1, 2015, pp. 1186-1189.

[21] Al-Gharbawi A., Decrease in failure load of inclined driven piles by using Allpile program, MATEC Web of Conferences, Vol. 162, 01010, 2018, pp. 1-10.

[22] Chiou J.S., Huang T.J., Chen C.L. and Chen C.H., Shaking table testing of two single piles of different stiffnesses subjected to liquefaction-induced lateral spreading, Engineering Geology, Vol. 281, 2021, 105956, pp. 1-10.

[23] Iai S., Similitude for Shaking table test on Soil-Structure-Fluid Model in 1g Gravitational Field, Soils and Foundations, Vol. 29, No. 1, 1989, pp. 105-118.

[24] Nagao T. and Shibata D., Experimental study of the lateral spreading pressure acting on a pile foundation during earthquakes, Engineering, Technology & Applied Science Research, Vol. 9, No. 6, 2019, pp. 5021-5028.

[25] Nagao T., An Experimental study on the way bottom widening of pier foundations affects seismic resistance, Engineering, Technology & Applied Science Research, Vol. 10, No. 3, 2020, pp. 5713-5718.

[26] Nagao T. and Tsutaba R., Evaluation Methods of Vertical Subgrade Reaction Modulus and Rotational Resistance Moment for Seismic Design of Embedded Foundations, Engineering, Technology & Applied Science Research, Vol. 11, No. 4, 2021, pp. 7386-7392.

[27] Nagao T., Effect of Foundation Width on Subgrade Reaction Modulus, Engineering, Technology & Applied Science Research, Vol. 10, No. 5, 2020, pp. 6253-6258.

[28] Suetomi I. and Yoshida N., Nonlinear Behavior of Surface Deposit during the 1995 Hyogoken-Nambu Earthquake, Soils and Foundations, Vol. 38, 1998, pp. 11-22.

[29] Jiang C., Zhang Z. and He J., Nonlinear analysis of combined loaded rigid piles in cohesionless soil slope, Computers and Geotechnics, Vol. 117, 2020, 103225, pp. 1-9.

[30] Nadilla S. and Prakoso W.A., Pile lateral subgrade reaction modulus for Jakarta, MATEC Web of Conferences, Vol. 270, 02002, 2019, pp. 1-6.

[31] Abd-Elhamed A., Analytical Solution of Laterally Loaded Free-Head Long Piles in Elasto-Plastic Cohesive Soils, Mathematics, Vol. 9, No. 16, 2021, pp. 1-13.

[32] Taheri O., Moayed R.Z. and Nozari M., Lateral Soil-Pile Stiffness Subjected to Vertical and Lateral Loading, Journal of Geotechnical and Transportation Engineering, Vol. 1, No. 2, 2015, pp. 30-37.